JOURNAL OF Applied Polymer SCIENCE

Preparation and Properties of Carbon Nanotube/Binary-Polymer Composites with a Double-Segregated Structure

Huan Pang,[1] Yu Bao,[1] Shu-Gui Yang,[1] Chen Chen,[1] Wei-Qin Zhang,[1] Jun Chen,[1] Xu Ji,[2] Jun Lei[1*]

[1]College of Polymer Science and Engineering and State Key Laboratory of Polymer Materials Engineering, Sichuan University, Chengdu, Sichuan 610065, People's Republic of China

[2]College of Chemical Engineering, Sichuan University, Chengdu, Sichuan 610065, People's Republic of China

Correspondence to: J. Lei (E - mail: leijun@scu.edu.cn)

ABSTRACT: A carbon nanotube (CNT)/poly(methyl methacrylate) (PMMA)/ultrahigh molecular weight polyethylene (UHMWPE) composite containing a double-segregated structure was formalized by means of a facile mechanical mixing technology. In the composite, the CNTs were decorated on the surfaces of PMMA granules, and the CNTs decorated granules formed the continuous segregated conducting layers at the interfaces between UHMWPE particles. Morphology observations confirmed the formation of a specific double-segregated CNT conductive network, resulting in an ultralow percolation threshold of ~0.2 wt %. The double-segregated composite containing only 0.8 wt % CNT loading exhibited a high electrical conductivity of ~0.2 S m^{-1} and efficient electromagnetic shielding effectiveness of ~19.6 dB, respectively. The thermal conductivity, temperature-resistivity behaviors, and mechanical properties of the double-segregated composites were also studied. This work provided a novel conductive network structure to attain a high-performance conducting polymer composite at low filler loadings. © 2013 Wiley Periodicals, Inc. J. Appl. Polym. Sci. 000: 000–000, 2013

KEYWORDS: composites; structure-property relations; polyolefins; nanotubes; graphene and fullerenes

Received 3 May 2013; accepted 22 July 2013; Published online

DOI: 10.1002/app.39789

INTRODUCTION

Carbon nanotube (CNT)-filled conductive polymer composites (CPCs) have been used in various electronic applications such as electrostatic discharge protection, electromagnetic shielding interference, sensor devices, and flexible electronics.[1–4] However, the CNT filled CPCs prepared by the conventional melt-mixing method generally have high conductive filler loadings for attaining a high electrical conductivity, causing a series of disadvantages.[5–7] For instance, a high filler loading (e.g. ~7 wt % CNT loading[8]) is often required for adequate electromagnetic interference (EMI) shielding capability (~20 dB) in conventional CNT-filled CPCs, which adversely affects the economic feasibility, processability, and mechanical properties. To date, it therefore remains a considerable challenge to reduce the CNT loading without compromising the high electrical conductivity.

Forming a segregated structure within the polymer composite is currently the most successful strategy for achieving the high electrical conductivity at low loading levels.[9–11] Zhao et al. fabricated a CNT/poly(vinylidene fluoride) composite with a segregated structure, and obtained an electrical conductivity of ~1 S m^{-1} at 0.4 wt % CNT loading. This is approaching the target conductivity of ~1 S m^{-1} desired for efficient EMI shielding effectiveness (EMI SE).[12] Yu et al. used the latex technology to manufacture a segregated CNT-poly(vinyl acetate) composite, attaining a high electrical conductivity of ~10^2 S m^{-1} at 5 wt % CNT loading, which is sufficient for majority of electronic devices.[13] Despite of high efficiency of segregated structure in forming conductive networks, as yet there are few reports concerning high-performance composite materials based on segregated CNT-filled CPCs.[14] In this study, we designed a facile methodology to prepare the double-segregated conducting composites, in which ultrahigh molecular weight polyethylene (UHMWPE) was employed to scaffold a segregated conductive network. The conductive network was composed from another segregated CNT structures localized at the interfaces between poly(methyl methacrylate) (PMMA) granules. The resulting composites exhibited the desirable electrical conductivity and EMI SE at low loading levels. Additionally, the thermal conductivity, temperature-resistivity behaviors, and mechanical properties of the double-segregated composites were also studied.

Additional Supporting Information may be found in the online version of this article.

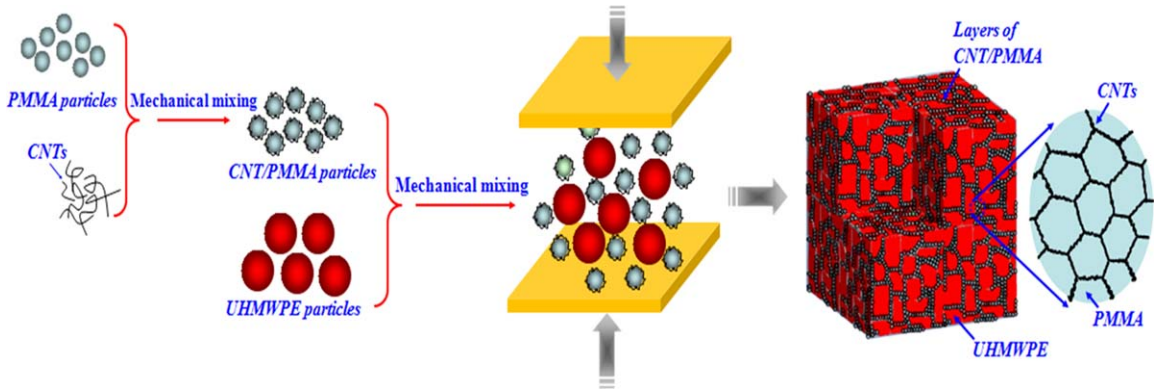

Figure 1. Schematic for the fabrication of the double-segregated CNT/PMMA/UHMWPE composites. [Color figure can be viewed in the online issue, which is available at wileyonlinelibrary.com.]

EXPERIMENTAL

Materials

The UHMWPE in powder with density of 0.94 g cm^{-3}, granular diameter of 210 μm, and weight-average-molecular weight of 6×10^6 g mol^{-1} was applied by Beijing No. 2 Auxiliary Agent Factory (Beijing, China). PMMA (SUMIPEX MH, number-average-molecular weight $M_n = 2.2 \times 10^4$ g mol^{-1}, density $\rho = 1.18$ g cm^{-3}, and glass temperature $T_g = 105°C$) was purchased from Sumitomo Chemical Corporation (Singapore). The PMMA granules with a diameter of ~20 μm were prepared by high-speed mechanical pulverization. Multiwalled CNTs (M510 provided by Chengdu Organic Chemicals, Chengdu, China), with an average diameter of 20–40 nm and a length of 10–20 μm, were used as the model electrically conductive fillers.

Composite Preparation

As illustrated in Figure 1, CNT : PMMA weight ratio of 1 : 19 were used to fabricate the conducting CNT/PMMA particles using the high-speed mechanical mixing. After that, the UHMWPE and 5 wt % CNT/PMMA particles were mixed uniformly in their solid state in a mechanical mixer, at a speed of 24,000 rmp. Finally, the granule mixtures of UHMWPE and CNT/PMMA particles were compression molded in a hot press for 5 min, under 10 MPa, at a temperature of 170°C, to form rectangular sheets ($70 \times 70 \times 0.5$ mm^3) for the following characterizations.

Characterizations

The optical micrograph was taken using Olympus BX51 optical microscopy (OM), about 15 μm thickness samples were microtomed at room temperature from the compression-molding sheets. Transmission electron microscopy (TEM) was performed on an FEI Tecnai F20, with an accelerating voltage of 200 kV. The thickness of the sample films was ~80 nm, as determined using a Leica EMUC6/FC6 microtome. For direct current electrical conductivity measurements, silver pastes were stuck to the surface of each sample to ensure good contact of the sample surface with the electrodes. The electrical resistance of the composites was measured using a Keithley 4200SCS apparatus. Thermal conductivity was measured by the transient plane source technique using a Hot Disk 2500-OT equipment (Hot disk AB, Sweden) at room temperature according to ASTM C518-91. Differential scanning calorimetry (DSC) measurement of CNT/PMMA/UHMWPE composites was carried out on a TA Instruments' Q200 under a nitrogen flow, which was calibrated by indium as the standard. In the resistivity-temperature test, the sample was immersed in silicone oil of a temperature-controlled apparatus to avoid oxidation. The thermal procedure of the sample for resistivity-temperature test was, heated from 20 to 180°C at 2°C min^{-1} and held at this temperature for 3 min, then cooled to 20°C at the same rate. The data were recorded by a computer. EMI SE of samples with 10 mm diameter and 2.5 mm thickness in the 8.2–12.4 GHz (X-band) frequency range was measured using Agilent vector network analyzer HP4291B (More detailed information was provided in Supporting Information). The tensile testing was carried out at room temperature, using an Instron universal test instrument (Model 5576, Instron Instruments, America) with a crosshead speed of 50 mm min^{-1}, and a gauge length of 20 mm. To evaluate the tensile modulus, a draw speed of 5 mm min^{-1} was applied.

RESULTS AND DISCUSSIONS

We first observed the double-segregated structure of the fabricated CPCs. As shown in Figure 2(a), the OM micrograph of the CNT/PMMA/UHMWPE composites provides the direct evidence for the formation of a typical segregated structure, in which the conducting CNT/PMMA layers surrounded the individual UHMWPE particles throughout the CPCs. Observing from TEM micrograph of Figure 2(b), the CNTs were localized at the interfaces between PMMA granules to create another segregated structure. The formation of such an interesting structure could be understood from its fabrication process. The low processing temperature and weak shear flow caused the UHMWPE particles and CNT/PMMA granules to remain largely intact and CNT surface moieties could not permeate into the polymer matrix during hot compaction. With the crystallization of UHMWPE matrix upon cooling, the continuous conducting CNT/PMMA pathways remained at the interface regions of UHMWPE particles, which experienced limited plastic deformation rather than viscous flow under pressure.[15]

The next concern was the transport behaviors of the double-segregated composites. We examined the electrical and thermal

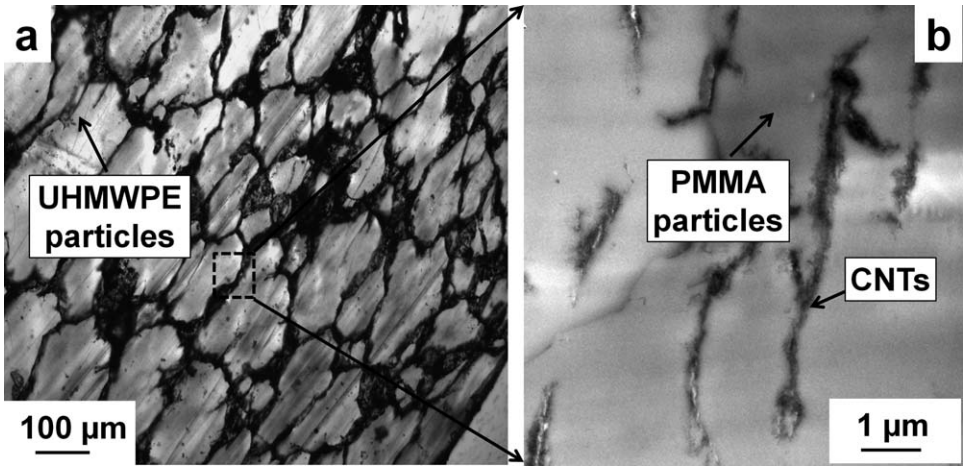

Figure 2. (a) OM micrograph of a CNT/PMMA/UHMWPE (1/19/80 by weight) film and (b) TEM micrograph of its film.

conductivity of CNT/PMMA/UHMWPE composites as a function of CNT mass concentration as shown in Figure 3. As expected, the electrical percolation threshold was found to be satisfactorily low (only 0.2 wt % CNT loading), which is very low CNT loading to make composites electrically conductive, indicative of high-efficiency of the double-segregated structure in forming conductive networks.[16] Moreover, it is noticeable that the 2 wt % CNT filled composite possessed an electrical conductivity of ~3 S m^{-1}, which is sufficient for some electrical applications (e.g., electrostatic discharge protection, electromagnetic shielding interference, and sensors).[17] The variation of thermal conductivity with CNT loadings is shown in Figure 3(b). The thermal conductivity of the double-segregated composites first increased and then anomalously decreased with increasing CNT content. The maximum thermal conductivity of 0.36 W mk^{-1} was reached at 0.8 wt % CNT, but was only 36% greater than that of the unfilled polymer matrix. This level of thermal conductivity enhancement felt well below the theoretical predictions in comparison with the superior intrinsic thermal conductivity of pristine CNTs.[18,19] The low value of thermal conductivity for CNT/PMMA/UHMWPE composites could be ascribed to the large interfacial thermal resistance between the contact spots of CNTs[19]; while the anomalous drop of thermal conductivity was due to the increasing levels of porosity and poor interaction between CNT and polymer matrix, which was also reported in other literature.[20,21]

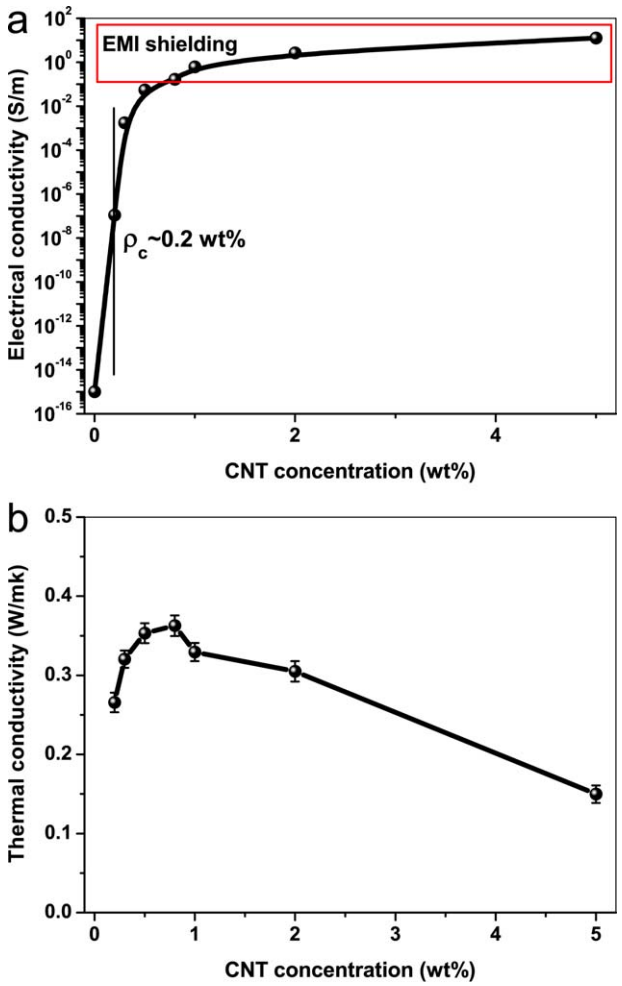

Figure 3. Electrical conductivity (a) and thermal conductivity (b) as a function of CNT content for the CNT/PMMA/UHMWPE composite with a double-segregated structure. [Color figure can be viewed in the online issue, which is available at wileyonlinelibrary.com.]

The temperature dependences of the volume resistivity in CNT/PMMA/UHMWPE composites during three heating-cooling runs (HCRs) are presented in Figure 4. In this measurement, the CNT loadings of the double-segregated composites were fixed at 0.3 and 0.5 wt %, both just beyond its percolation threshold (0.2 wt %) to guarantee the double-segregated structure highly sensitive to the temperature field, and made the resistivity-temperature behaviors of these two composites comparable (In addition, if the CNT loading of CPC was below 0.3 wt %, the volume resistivity was too high to be recorded by our apparatus). The double-segregated CNT/PMMA/UHMWPE composites both experienced a positive temperature coefficient (PTC) effect around the melting point of UHMWPE followed by a negative temperature coefficient (NTC) phenomenon. In the first cycle of 0.3 wt % CNT/PMMA/UHMWPE composites, the volume resistivity started increasing at 110°C during heating, and arrived at the maximal value at 137°C, while during

Applied Polymer SCIENCE

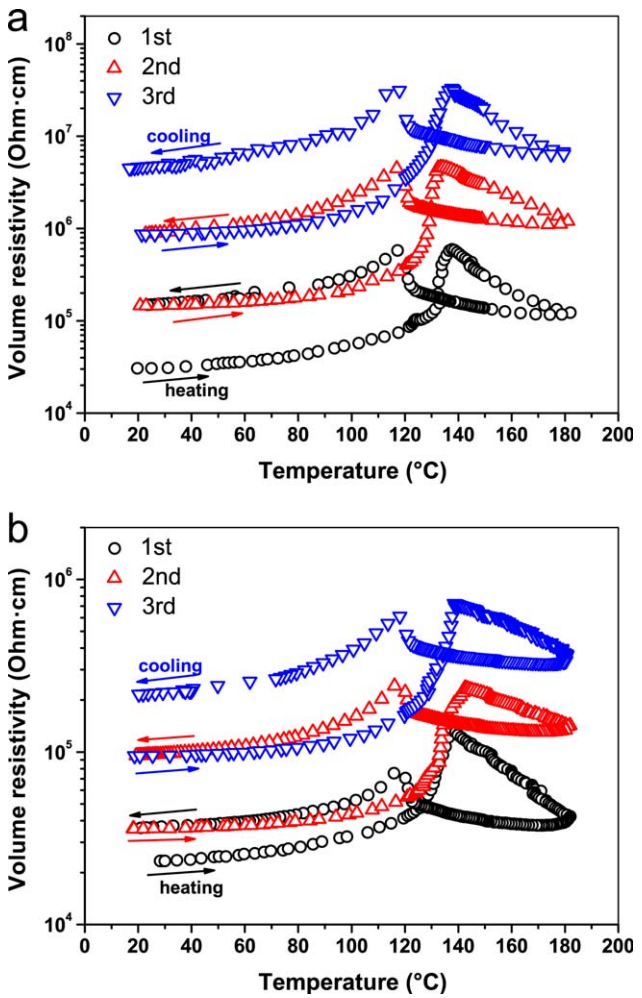

Figure 4. Resistivity temperature behaviors of 0.3 wt % (a) and 0.5 wt % (b) CNT/PMMA/UHMWPE composites in three HCRs. [Color figure can be viewed in the online issue, which is available at wileyonlinelibrary.com.]

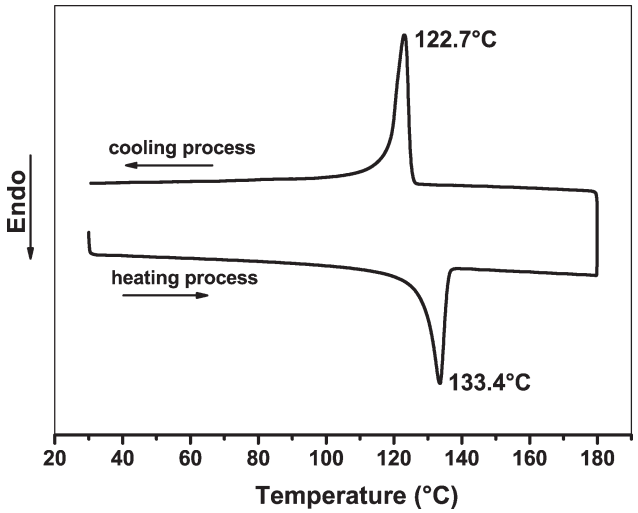

Figure 5. DSC scans of 0.3 wt % CNT/PMMA/UHMWPE composites at a heating and cooling rate of 2°C min^{-1}.

cooling the volume resistivity begun to rise dramatically from about 120°C. The rapid increase of the volume resistivity during HCRs was in full agreement with the melting and crystallization behaviors of CNT/PMMA/UHMWPE composites estimated from the DSC curves as shown in Figure 5, which showed the melting point of UHMWPE matrix was 133.4°C and the maximal crystallization temperature was 122.7°C. The temperature-resistivity behavior of the 0.5 wt % CNT/PMMA/UHMWPE composite was similar with that of the 0.3 wt % CNT one.

Figure 6 depicts the morphology evolution for the double-segregated CNT/PMMA/UHMWPE composites during the first HCRs. With the elevated temperature, the segregated CNT conducting pathways became vulnerable and the gaps between CNTs increased because of the different thermal expansion coefficient between CNTs and PMMA matrix, resulting in a moderate increase of volume resistivity [Figure 4(b)]. When the temperature rose around the melting point of UHMWPE, its crystallites started to melt. The transformation of the crystalline phase into the amorphous phase caused the conducting CNT/PMMA layers diffusing randomly on the UHMWPE granule surfaces, corresponding to the disconnection of some conducting double-segregated pathways [see Figure 6(c)].

With an abrupt increase in the volume resistivity, a PTC phenomenon took place. The PTC intensity (I_{PTC}), was defined as: $I_{PTC} = \log (R_P/R_{TR})$, where R_P was the maximum resistivity in heating journey, R_{TR} was the original resistivity at room temperature. I_{PTC} of CNT/PMMA/UHMWPE composites was 1.29, 1.48, and 1.58, respectively from the first to third cycles for the 0.3 wt % CNT/PMMA/UHMWPE sample, and 0.77, 0.82, and 0.88 for the 0.5 wt % CNT one. Noticeably, the value of I_{PTC} was relatively low compared with conventional melt-mixing CPCs.[22–24] As shown in Figure 6(c), the CNT agglomerates could not easily immigrate into polymer matrix because of the segregated location of conducting component and high melt-viscosity of polymer matrix, only diffusing along the polymer granular interfaces. Thus, the double-segregated conductive network of CNTs did not change pronouncedly during the heating journey. It is also demonstrated from Figure 6(c) that the double-segregated conductive architecture survived from the ambient high temperature of 180°C. Additionally, the melt-viscosity of UHMWPE due to the excessive entanglement of UHMWPE chains was so high that the conducting CNT/PMMA layers was also difficult to penetrate into the UHMWPE matrix and was only squeezed at the interface between UHMWPE particles, so the increase of the tube-tube gap was limited. Both of the two factors led to the relatively low I_{PTC}.

The NTC phenomenon took place when CNTs begun to aggregate at the interface of polymer matrix to recover the conducting CNT pathways in the melt state. The high melt-viscosity of the double-segregated composites restricted the reorganization of the double-segregated conductive network, causing an obvious NTC intensity. With the test temperature dropping from 180°C, the volume resistivity rose slowly because of cooling process inducing the higher viscosity of the double-segregated CPC, which hindered CNTs from aggregating to form perfect conducting CNT channels [see Figure 6(d)]. When

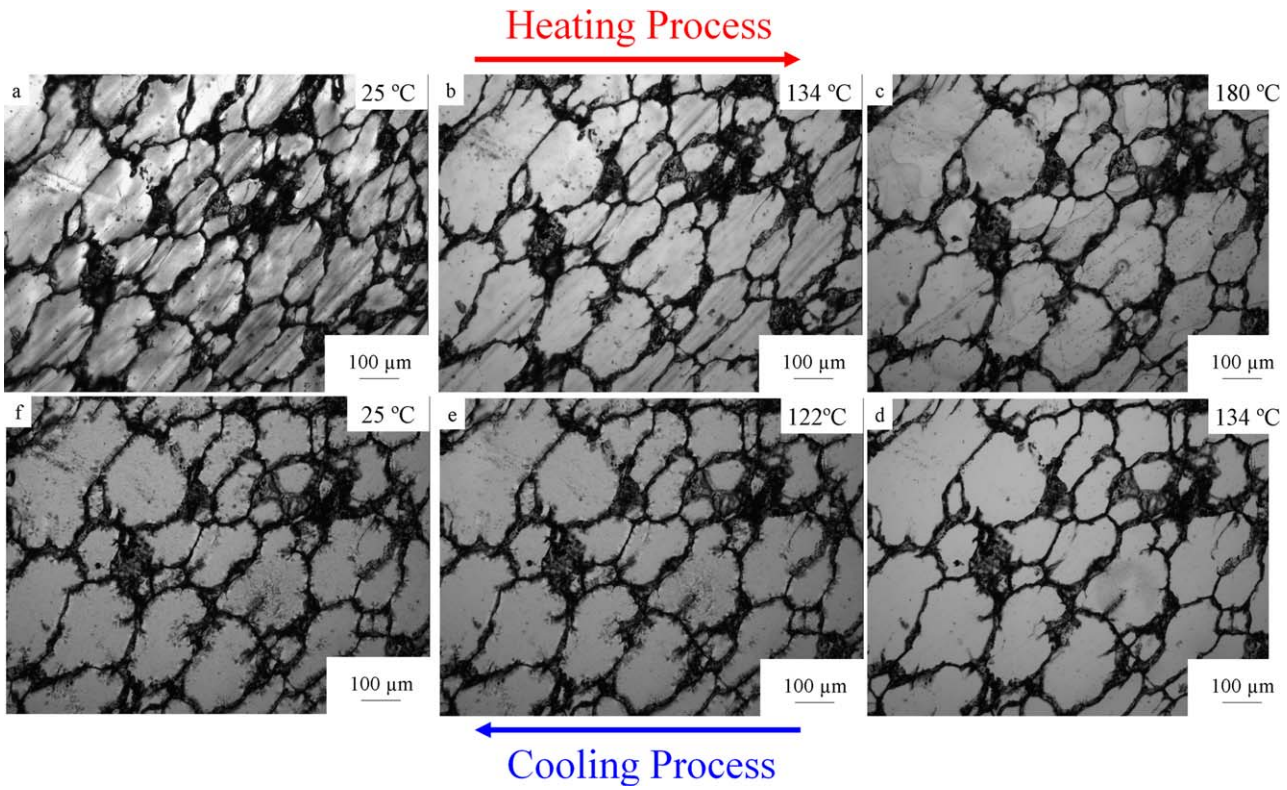

Figure 6. OM images of 0.5 wt % CNT/PMMA/UHMWPE composites in the first cycles at a heating and cooling rate of 2°C min^{-1}. [Color figure can be viewed in the online issue, which is available at wileyonlinelibrary.com.]

the temperature was lower the UHMWPE melting temperature, UHMWPE phase started to crystallize. The percolated CNT/PMMA component was ejected from the UHMWPE crystalline regions and concentrated in the amorphous regions [see Figure 6(e)]. Therefore, the conducting CNT channels were gradually broken up, resulting in the increase of the volume resistivity.

After returning to the room temperature, the volume resistivity of the double-segregated CNT/PMMA/UHMWPE composites became a little larger than the initial one, same result with our previous studies on the temperature dependence of volume resistivity for CNT/polyethylene composites,[25] and the second and third curves shifted upward in comparison with the first cycle. This phenomenon was ascribed to the initial and final state of the double-segregated composites was a little different from each other [Figures 6(a,f)]. Owing to the intense Brownian motion and crystallization induced flow, the segregated conducting CNT/PMMA layers was much thicker than the original layer, and the conductive CNT/PMMA layers were less densely packed compared to those of the original composites. Moreover, the double-segregated conductive network might be weaker than the common three-dimension conductive network, so it did not recover to the original condition, leading to a higher volume resistivity.

EMI SE is a measure of the capacity of materials to attenuate EMI wave intensity.[26] For the conventional CPC-based materials, an efficient EMI shielding performance usually needs a high electrical conductivity (usually >1 S m^{-1}).[27] In this work, the CNT loadings above the percolation threshold were incorporated into the double-segregated CNT/PMMA/UHMWPE composites. As shown in Figure 3(a), the electrical conductivity of samples with 0.8, 1.0, and 2.0 wt % CNT loadings, which were ~0.2, 0.6, and 2.8 S m^{-1}, respectively. Despite the low CNT loadings, the electrical conductivity of the double-segregated CNT/PMMA/UHMWPE composites met the requirement of EMI materials. The electrical conductivity was comparable at these three loadings, likely because of the saturation of electron transfer in CNT pathways, since the CNT concentration of CNT/PMMA was fixed at 5 wt %.

The variation of EMI SE over X band for the double-segregated CNT/PMMA/UHMWPE composites with various CNT loading is shown in Figure 7(a). It is observed that the EMI SE of the double-segregated composite was almost independent of the frequency in the measured frequency region. The average EMI SE of the 0.8, 1.0, and 2.0 wt % CNT loading samples (2.5 mm in thickness) was measured to be 19.6, 19.7, and 19.8 dB, respectively, over a frequency of 8.2–12.4 GHz. The specific EMI SE (the ratio of EMI SE to conducting filler loading) was used to evaluate the shielding performance, since EMI SE and economic feasibility are both limited by the incorporation of conductive fillers. In our study, it is worth noting that the average specific EMI SE of the double-segregated composite containing 0.8 wt % CNTs was as high as 25 dB·(wt %)$^{-1}$. The efficient EMI shielding by the double-segregated composite at relatively low CNT loadings was attributed mainly to the formation of the double-segregated nanotube networks between the insulating polymer matrixes. The EMI SE independence of CNT loading

Applied Polymer SCIENCE

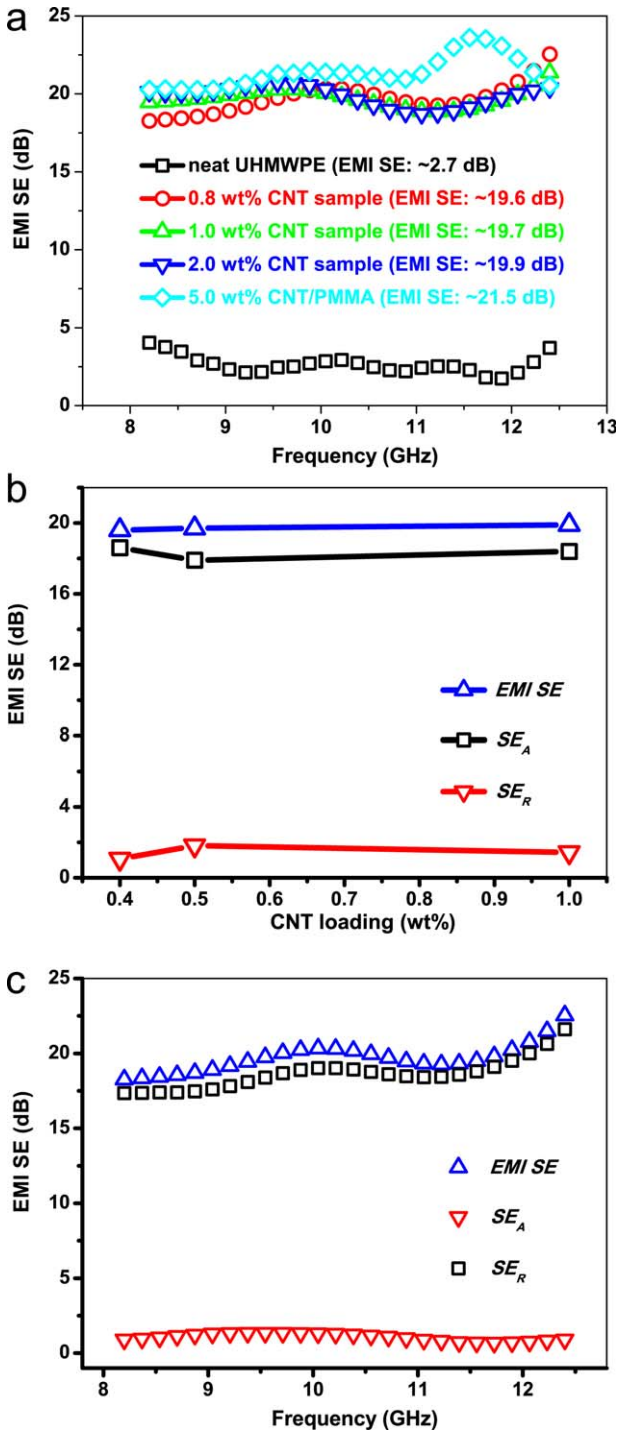

Figure 7. (a) EMI SE in the X band of the CNT/PMMA, neat UHMWPE and double-segregated composites. (b) Comparison of average EMI SE, SE_A, and SE_R at various CNT loadings. (c) Comparison of EMI SE, SE_A, and SE_R for the double-segregated composite with 0.8 wt % CNT loading. [Color figure can be viewed in the online issue, which is available at wileyonlinelibrary.com.]

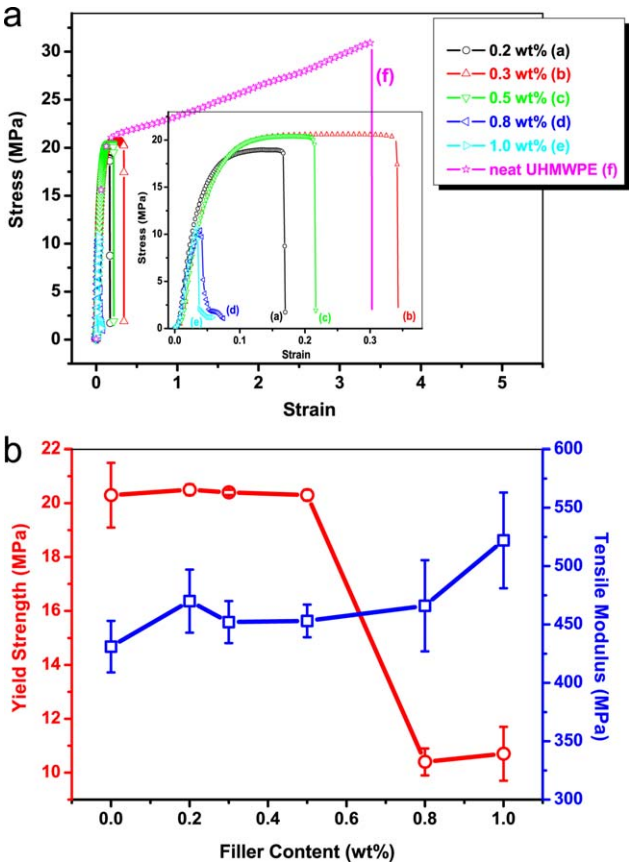

Figure 8. (a) Typical stress-strain curves for the CNT/PMMA/UHMWPE composites. (b) Yield strength and modulus of CNT/PMMA/UHMWPE composites with various CNT loadings. [Color figure can be viewed in the online issue, which is available at wileyonlinelibrary.com.]

was ascribed to the maximum density of conducting CNT pathways having been reached in the segregated CNT/PMMA layers. In other words, the EMI SE of the double-segregated composites could not be improved at higher CNT/PMMA loadings, since its EMI capability was limited because of the fixed CNT content in the percolated CNT/PMMA layers, the average EMI SE of which was ~21.5 dB.

To clarify the EMI shielding mechanism of the double-segregated composite, the average EMI SE, microwave absorption (SE_A) and microwave reflection (SE_R) were estimated, as shown in Figure 7(b). The contribution from microwave reflection was negligible compared with the strong absorption of electromagnetic energy. For example, the average SE_R and SE_A for the 0.8 wt % CNT sample were ~1 and 18.6 dB, respectively [Figure 7(c)]. This indicated the formation of an effective double-segregated conducting network containing extensive conducting CNT paths within the CNT/PMMA layers, which favored the multiabsorption and attenuation of electromagnetic waves by conductive dissipation.[28]

In the next section, we discussed the tensile behaviors of the double-segregated composites, as shown in Figure 8. Figure 8(a) illustrates the representative stress-strain curves of the double-segregated CNT/PMMA/UHMWPE composites and neat UHMWPE. Pure UHMWPE shows a ductile fracture with a strain-at-failure of about 340%. After adding the percolated CNT/PMMA component to the UHMWPE matrix, the composite strain decreased significantly below 50%. The yield strength

and tensile modulus of the double-segregated composites were obtained from the curves and are summarized in Figure 8(b). The yield strength exhibited a general trend: the properties leveled off at a certain value of ~20 MPa and then decreased to only 10 MPa at a critical CNT content of 0.8 wt %. The degradation of yield strength may have originated from three factors; (1) the poor compatibility between PMMA and UHMWPE domains, (2) the agglomeration state of CNTs, and (3) weaker adhesive interaction between the polymer granules.[7,29,30] However, the tensile modulus of the double-segregated composites showed a moderate increase, from 431 MPa for pure UHMWPE, to 522 MPa for 1.0 wt % CNT/PMMA/UHMWPE bars, because of the reinforcement of CNTs in the conducting CNT/PMMA layers.

CONCLUSION

In summary, we fabricated a double-segregated conductive polymer composite, in which the continuous segregated conducting CNT/PMMA layers localized at the interfaces of UHMWPE granules to form another segregated conductive network. The double-segregated composite exhibited a high electrical conductivity, invariable thermal conductivity, low temperature-resistivity intensity, and efficient EMI performance at relatively low CNT loadings. The degradation of mechanical properties was ascribed to the poor compatibility between PMMA and UHMWPE domains and the agglomeration of CNTs in the double-segregated structure. This work also provided a new guideline for the easy fabrication of a high-performance CNT based CPC materials at low loading levels.

ACKNOWLEDGMENTS

The work was funded by the National Natural Science Foundation of China (Contract No. 21276168, 51273131 and 21176158) for financial support. The authors appreciated the financial support from Sichuan Province Science and Technology Support Program (2012RZ0004).

REFERENCES

1. Bauhofer, W.; Kovacs J. Z. *Compos. Sci. Technol.* **2009**, *69*, 1486.
2. Rangari, V. K.; Samsur, R.; Jeelani, S. *J. Appl. Polym. Sci.* **2013**, *129*, 1249.
3. Arronche, L.; Saponara, V. L.; Yesil, S.; Bayram, G. *J. Appl. Polym. Sci.* **2013**, *128*, 2797.
4. Dang, Z. M.; Yuan, J. K.; Zha, J. W.; Zhou, T.; Li, S. T.; Hu, G. H. *Prog. Mater. Sci.* **2012**, *57*, 660.
5. Bao, H. D.; Sun, Y.; Xiong, Z. Y.; Guo, Z. X.; Yu, J. *J. Appl. Polym. Sci.* **2012**, *128*, 735.
6. Geetha, S.; Satheesh, K. K.; Chepuri, R.; Rao, K.; Vijayan, M.; Trivedi, D. C. *J. Appl. Polym. Sci.* **2009**, *112*, 2073.
7. Pang, H.; Yan, D. X.; Bao, Y.; Chen, J. B.; Chen, C.; Li, Z. M. *J. Mater. Chem.* **2012**, *22*, 23568.
8. Yang, Y. L.; Gupta, M. C.; Dudley, K. L.; Lawrence, R. W. *Nano. Lett.* **2005**, *5*, 2131.
9. Wang, D. R.; Zhang, X. M.; Zha, J. W.; Zho, J.; Dang, Z. M.; Hu, G. H. *Polymer* **2013**, *54*, 1916.
10. Pang, H.; Chen, T.; Zhang, G. M.; Zeng, B. Q.; Li, Z. M. *Mater. Lett.* **2010**, *64*, 2226.
11. Grunlan, J. C.; Mehrabi A. R.; Bannon, M. V.; Bahr J. L. *Adv. Mater.* **2004**, *16*, 150.
12. Liu, Q. M.; Tu, J. C.; Wang, X.; Xu, W. X.; Zheng, W. T. Zhao, Z. D. *Carbon* **2012**, *50*, 339.
13. Yu, C.; Kim, Y. S.; Kim, D.; Grunlan, J. C. *Nano. Lett.* **2008**, *8*, 4428.
14. Pang, H.; Chen, C.; Bao, Y.; Chen, J.; Ji, X.; Lei, J.; Li, Z. M. *Mater. Lett.* **2012**, *79*, 96.
15. Pang, H.; Piao, Y. Y.; Tan, Y. Q.; Jiang, G. Y.; Wang, J. H.; Li, Z. M. *Mater. Lett.* **2013**, *107*, 150.
16. Pang, H.; Bao, Y.; Xu, L.; Yan, D. X.; Zhang, W. Q.; Wang, J. H.; Li Z. M. *J. Mater. Chem. A* **2013**, *1*, 4177.
17. Al-Saleh, M.; Sundararaj, U. *Carbon* **2009**, *47*, 2.
18. Nan, C. W.; Shi, Z.; Lin, Y. *Chem. Phys. Lett.* **2003**, *375*, 666.
19. Grunlan, J. C.; Kim, Y. S.; Ziaee, S.; Wei, X.; Abdel-Magid, B.; Tao, K. *Macromol. Mater. Eng.* **2006**, *291*, 1035.
20. Nan, C. W.; Liu, G.; Lin, Y.; Li, M. *Appl. Phys. Lett.* **2004**, *85*, 3549.
21. Huxtable, S. T.; Cahill, D. G.; Shenogin, S.; Xue, L.; Ozisik, R.; Barone, P.; Usrey, M.; Strano, M. S.; Siddons, G.; Shim, M.; Keblinski, P. *Nat Mater* **2003**, *2*, 731.
22. Pang, H.; Zhang, Y. C.; Chen, T.; Zeng, B. Q.; Li, Z. M. *Appl. Phys. Lett.* **2010**, *96*, 251907.
23. Zhang, C.; Ma, C. A.; Wang, P.; Sumita, M. *Carbon* **2005**, *43*, 2544.
24. Lisunova, M. O.; Mamunya, Y. P.; Lebovka, N. I.; Melezhyk A. V. *Eur. Polym. J.* **2007**, *43*, 949.
25. Pang, H.; Chen, Q. Y.; Bao, Y.; Yan, D. X.; Zhang, Y. C.; Chen, J. B.; Li, Z. M. *Plast. Rubber Compos.* **2013**, *42*, 59.
26. Gelves, G. A.; Al-Saleh, M. H.; Sundararaj, U. *J. Mater. Chem.* **2011**, *21*, 829.
27. Zhang, H. B.; Yan, Q.; Zheng, W. G.; He, Z. X.; Yu, Z. Z. *ACS Appl. Mater. Interfaces* **2011**, *3*, 918.
28. Thomassin, J. M.; Huynen, I.; Jerome, R.; Detrembleur, C. *Polymer* **2010**, *51*, 115.
29. Ma, P. C.; Liu, M. Y.; Zhang, H.; Wang, S. Q.; Wang, R.; Wang, K.; Wong, Y. K.; Tang, B. Z.; Hong, S. H.; Paik, K. W.; Kim, J. K. *ACS Appl. Mater. Interfaces* **2009**, *1*, 1090.
30. González, I.; Eguiazábal, J. I.; Nazabal, J. *Compos. A* **2012**, *43*, 1482.